sustainability

MDPI

Article

Numerical Analysis of Low-Enthalpy Deep Geothermal Energy Extraction Using a Novel Gravity Heat Pipe Design

Urban Gselman [1], Vid Peršak [2] and Darko Goričanec [1,*]

[1] Faculty of Chemistry and Chemical Engineering, University of Maribor, Smetanova ulica 17, 2000 Maribor, Slovenia; urban.gselman@student.um.si
[2] Faculty of Computer and Information Science, University of Ljubljana, Večna pot 113, 1000 Ljubljana, Slovenia; vp5902@student.uni-lj.si
* Correspondence: darko.goricanec@um.si

Abstract: Geothermal energy, derived from the Earth's internal heat, can be harnessed due to the geothermal gradient between the Earth's interior and its surface. This heat, sustained by radiogenic decay, varies across regions, and is highest near volcanic areas. In 2020, 108 countries utilised geothermal energy, with an installed capacity of 15,950 MWe for electricity and 107,727 MW_t for direct use in 2019. Low-enthalpy sources require binary systems for power production. Open-loop systems face issues like scaling, difficult water treatment, and potential seismicity, while closed-loop systems, using abandoned petroleum or gas wells, reduce costs and environmental impacts greatly. The novel geothermal gravity heat pipe (GGHP) design eliminates parasitic power consumption by using hydrostatic pressure for fluid circulation. Implemented in an abandoned well in north-east (NE) Slovenia, the GGHP uses a numerical finite difference method to model heat flow. The system vaporises the working fluid in the borehole, condenses it at the surface, and uses gravitational flow for circulation, maintaining efficient heat extraction. The model predicts that continuous maximum capacity extraction depletes usable heat rapidly. Future work will explore sustainable heat extraction and potential discontinuous operation for improved efficiency.

Keywords: geothermal energy; geothermal gravity heat pipe; numerical modelling; single-well closed-loop heat exchanger

Citation: Gselman, U.; Peršak, V.; Goričanec, D. Numerical Analysis of Low-Enthalpy Deep Geothermal Energy Extraction Using a Novel Gravity Heat Pipe Design. *Sustainability* **2024**, *16*, 6660. https://doi.org/10.3390/su16156660

Academic Editors: Chen Cao, Wen Zhang, Jie Dou and Peihua Xu

Received: 28 May 2024
Revised: 16 July 2024
Accepted: 31 July 2024
Published: 3 August 2024

1. Introduction

Geothermal energy is the heat energy of the Earth that can be harnessed due to the temperature difference or geothermal gradient between the Earth's interior and its surface [1]. The temperature difference is due to the heat stored in the planet's core since the time of formation. This thermal battery is recharged further by the radioactive decay of elements in the crust and mantle. The heat released, called radiogenic heat, contributes a significant fraction, up to 88%, of the heat flux at the surface [2]. The geothermal gradient is not constant over the entire surface of the Earth but depends on the geological and geophysical parameters of individual areas. The highest gradient is generally found near or at volcanically active areas [3]. Otherwise, the average surface heat flux measures 70.9 mW/m^2 [4]. This heat was used by 108 countries worldwide in 2020, as reported by the World Geothermal Congress, with a total installed electrical capacity of 15,950 MW_e [5]. For the direct use of this heat, the approximation for 2019 is valid, where a total installed power of 107,727 MW_t was assumed [6]. Most of the currently unused geothermal potential is represented by low-enthalpy sources or sources with geothermal fluid temperatures lower than 150 °C [3,7]. A binary system is utilised for power production from these sources. The extracted geothermal fluid is usually not suitable to be discharged to the environment and is treated before being reinjected into the ground, which replenishes the underground reservoir and keeps the extraction sustainable. This incurs some technical risks, such as continuous scaling on the insides of pipes, difficult water treatment, and possible induced seismicity,

if the porosity of the geothermal field needs to be improved, as is conducted in enhanced geothermal systems [8]. If the geothermal fluid contains a significant amount of dissolved gases, those usually need to be separated from the fluid before reinjection and are released to the environment, making geothermal energy less environmentally benign than advertised [9].

Alternatively, a closed-loop system could be designed that does not use geothermal fluid as the energy carrier, evading all the disadvantages of the open-loop systems. Additionally, abandoned petroleum wells could be used instead of new drilling projects. The availability of existing thermophysical data that are logged for the petroleum industry and the now unnecessary drilling would reduce the high investment costs that are associated with low-enthalpy geothermal systems greatly [10], which would, in turn, lower its levelised cost of electricity (LCOE) value.

Alimonti et al. [11] did an extensive analysis on the existing literature describing either technology, implementation, or modelling approaches to closed-loop wellbore heat exchangers (WBHX), either with existing or newly drilled wells. The heat is extracted using a coaxial heat exchanger, where a working fluid is pumped in the annulus, gathering heat during its travel towards the bottom and returning to the surface in the central insulated pipe. The main parameters defining the effectiveness of heat extraction using WBHX are the thermal conductivity of the inner pipe, the fluid flow dynamics, and the geothermal heat flux in the surrounding formation [12]. As the heat is exchanged only through conduction over a relatively small surface area, the extracted heat is insufficient for power production in hydrothermal systems compared to traditional open-loop geothermal power plants [10]. Alternatively, the WBHX has a lower environmental impact, avoids many risks, and has a lower barrier for investment compared to open-loop systems. These traits might outweigh the disadvantages and could be a promising future alternative to classical systems, as there is an enormous amount of abandoned petroleum wells, with their number increasing over the course of society's decarbonisation [13].

Alternatively, a U-heat exchanger could be used, where one pipe is used to inject the working fluid into the system, while another is used for extraction. This technology is less researched and used mostly with two separate boreholes that are connected at the bottom [14]. High heat flows between the inlet and outlet of the heat exchanger prevent the design from being used in a single well case [15]. The working fluid then either exchanges heat with a secondary working fluid at the top or is involved directly in an organic Rankine cycle (ORC) on the surface [16].

All the above-mentioned designs use a pump for generating the required pressures and flows to induce a flow in the working fluid, which incurs parasitic power consumption, making the system less efficient. This and many other techno-economic factors plague the field, making the International Energy Agency recommend research into alternative and more sustainable solutions for geothermal energy extraction [17]. A novel and patented design, named GGHP, could be a solution, as it removes the parasitic power that is needed to circulate the working fluid and, instead, uses a hydrostatic pressure generated by the returning condensate to induce flow [18].

The GGHP concept and its implementation in an abandoned well in NE Slovenia will be described in this work, which is a part of a pilot geothermal power plant project [19]. A numerical finite difference method approximation of a two-dimensional nonstationary heat flow in an infinite medium with negligible surface resistance is employed to estimate the heat flow after 10 years of operation.

2. Materials and Methods

2.1. Geothermal Gravity Heat Pipe

The GGHP works by vaporising the working fluid in a section of the borehole and later condensing it at the top and returning it to the well as a liquid. The circulation is conducted by gravitational flow and a hydrostatic pressure created by the liquid column in the inlet tubing. Additionally, a condenser at the surface now becomes an indispensable part of the design, as it creates a pressure difference from the bottom of the borehole to the top, and

creates the liquid column that replenishes the borehole heat exchange zone. The pressure in the borehole–heat exchanger system is controlled by the amount of the working fluid in the system, the mass flow is regulated by the heat flow at the condenser, and the maximum temperature is set by the design specifics of the well installation and geothermal gradient in the surroundings. The working fluid needs to be selected according to its phase diagram, the density of its vapour fraction and consequential pressure drop from the heat exchange zone to the surface, and the thermal characteristics of the geothermal well in question.

The studied concept and its horizontal and vertical cross-section can be seen in Figure 1. An existing and cased borehole is fitted with two packers, packers 9 and 7, and a wellhead 18, which divide the borehole into two distinct zones: a heat exchange zone 14 and a vacuum-insulated zone 5. The location of packer 9 is determined by the designed liquid–vapour transition temperature of the working fluid and the local temperature gradient in the surrounding formation. It needs to be deep enough for the working fluid to be able to create a high enough liquid column and a consecutive hydrostatic pressure to create an effective vapour barrier. The packer is pierced by pipe 16 and pipe 17, which are the inlet and outlet pipe, respectively. At the end of the inlet pipe, a diffusor 6 is installed, which, together with the flow and hydrostatic pressure of the liquid working fluid, prevents the vapour fraction of the working fluid from exiting the borehole through the inlet tubing. This is the most defect-prone part of the system and needs to be designed with every possible failure point in mind. The two packers are inserted in a leak-tight manner, according to relevant standards and manufacturer instructions. The liquid fluid is introduced into zone 14 through the inlet tubing 16. In zone 14, the fluid vaporises, causing it to rise to the top of the zone and, consequently, to the surface through a wider diameter outlet pipe 17. The pressure drops because of irreversible vapour flow and makes the working fluid at the surface always a saturated steam phase. The fluid then produces usable work through an expansion step in a turbine and is later condensed fully, either by dry condensation or by exchanging heat with a secondary fluid through a full condensation step at the condenser.

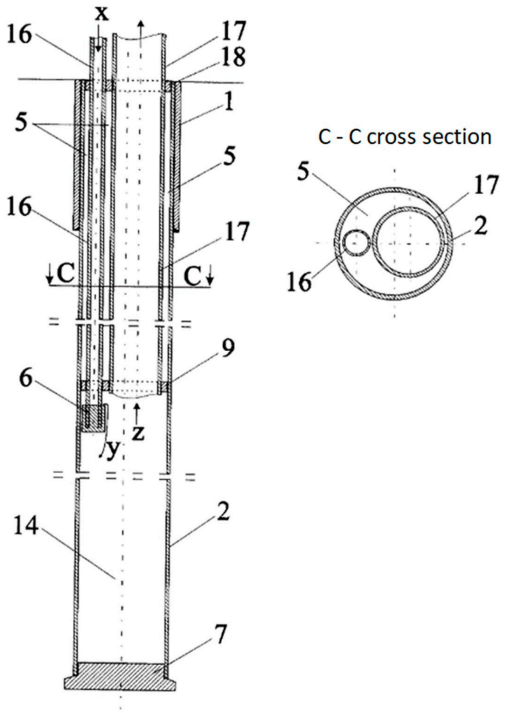

Figure 1. Vertical and horizontal cross-section of the analysed patented GGHP concept [18], reproduced without modifications and with permission from the authors. x, y, and z: flow direction of the working fluid. 1: outer casing. 2: inner casing. 5: vacuum-insulated zone. 6: vapour barrier. 7, 9, and 18: packers dividing the borehole in distinct zones. 14: heat exchange zone. 16: liquid inlet pipe. 17: vapour outlet pipe.

With careful balancing, considering the site specifics, choosing the right working fluid and good implementation, the design can work without any parasitic power consumption and without irreversibility losses on unnecessary valves. Because of the long reaction times of any changes to the main operating parameters during operation and a design that needs to consider site specifics for optimal production, an adequate model of the geothermal field and subsequent heat extraction needs to be made for the implementation to deliver the expected results.

2.2. Model Description

The temperature of the surrounding formation of the wellbore is described by an equation for nonstationary heat flow in an infinite medium with negligible surface resistance [20]. It was assumed that the thermal conductivity of the steel casing and the convection heat transfer coefficient from the casing to the working fluid is considerably higher than the thermal conductivity of the surrounding earth and can thus be neglected. Because the analysed well is a single well, two of the dimensions are symmetrical and the system can be reduced to two spatial dimensions, depth and distance from the borehole. The following is an equation of nonstationary heat flow in an infinite medium with negligible surface resistance in two dimensions:

$$\frac{\partial T}{\partial t} = \alpha \left(\frac{\partial^2 T}{\partial r^2} + \frac{\partial^2 T}{\partial z^2} \right) \tag{1}$$

$$\alpha = \frac{k}{\rho c_{\mathrm{p}}} \tag{2}$$

where T is the temperature dependent on time t and position/distance from the surface z and from the centre of the borehole r. α is the thermal diffusivity of the ground, with k, ρ, and c_{p} being its thermal conductivity, density, and specific heat capacity, respectively. The working fluid physical and thermal flow inside of the well was not modelled, as most of the heat is consumed for the working fluid phase transition, instead of its heating to transition temperature. The vapourisation temperature of the working fluid inside the heat exchange zone is not constant and increases with increasing depth, as the hydrostatic pressure of the gas column above increases the pressure below and the vapourisation temperature as a result.

A finite difference method was used for the numerical approximation of Equation (1), resulting in the following equation:

$$T_{i,\,j}^{n+1} = T_{i,\,j}^{n} + \alpha \Delta t \left(\frac{T_{i+1,\,j}^{n} + T_{i-1,\,j}^{n} - 2T_{i,\,j}^{n}}{\Delta r^2} + \frac{T_{i,\,j+1}^{n} + T_{i,\,j-1}^{n} - 2T_{i,\,j}^{n}}{\Delta z^2} \right) \tag{3}$$

where n, i, and j denote a single time, depth, or radial distance step Δt, Δz, and Δr, respectively. The equation compares the temperature of a point and the temperatures of its immediate surrounding points at a time step and calculates the resulting temperature, which is reused at the next time step. The stability of the equation and convergence of results is dependent on the three finitely approximated differences, where smaller distance steps and larger time steps make the equation unstable, resulting in positive and negative infinities [21]. The relationship between different step values and equation stability is outside of the scope of this paper. To shorten the calculation time as much as possible without making the equation unstable, the time steps were determined empirically and extended progressively from the starting 10^3 s up to 3.5×10^3 s.

The temperature in the undisturbed ground, before heat extraction has taken place, is described by a uniform heat gradient Γ:

$$T_j = T_0 + \Gamma z_j \tag{4}$$

where T_j denotes the temperature at depth j. The temperature surrounding the borehole during extraction is assumed to remain constant a sufficient distance away from the borehole. This limit is described as the distant field radius, or r_∞, and is described by the following equation [22]:

$$r_\infty = 4\sqrt{\alpha t_n} \tag{5}$$

where t_n is equal to the timeframe of the analysed extraction period.

In the case of GGHP technology, the heat extracted from the geothermal well is regulated by the working fluid mass flow rate, as the vapourisation temperature is fixed by the mass of the working fluid in the system. To calculate the extracted heat flow, the inside of the borehole is assumed to be thermally and physically equal to the surrounding formation, just at a temperature equal to the phase transition temperature of the working fluid. The inside of the well is permitted to heat up at each time step, and heat flow is calculated by comparing between the set temperature and the calculated temperature from Equation (3) with the following equation:

$$\phi = \frac{\rho c_\mathrm{p} \Delta z r_\mathrm{B}^2 \pi}{4\Delta t}\left(T_\mathrm{B}^{n+1} - T_\mathrm{B}^{n}\right) \tag{6}$$

where ϕ is the heat flow extracted from the borehole, r_B is the well casing outer radius, and T_B is the temperature in the borehole from the n and $n + 1$ time step. After the heat flow calculation, the borehole temperature is set back to the vapourisation temperature for the next time step, simulating minimal heat resistance of the iron casing and solid–gas interface compared to the surrounding formation.

2.3. Location Description and Parameters

An existing and abandoned research well in NE Slovenia named Pg-8 was chosen for the GGHP installation. The borehole data were provided by Petrol Geo d.o.o. The data for the surrounding rock formation are available from GeoZS, Slovenia's national geological survey organisation [23], and also articles that analysed earth samples and simulated the underground rock formation of the area [24,25]. The properties of the well and the surrounding rock are presented in Tables 1 and 2.

Table 1. Rock formation parameters surrounding the well, gathered from [24,25].

Parameter	Value
Thermal conductivity of the surrounding formation k (W m^{-1} K^{-1})	3
Density of the formation ρ (kg m^{-3})	2600
Formation heat capacity c_p (J kg^{-1} K^{-1})	800
Temperature gradient Γ (K m^{-1})	0.04
Formation temperature at 1st packer (°C)	60

Table 2. Well and installation parameters, supplied by the land and borehole owner Petrol Geo d.o.o.

Parameter	Value
Well casing outer diameter (m)	0.2445, 0.1778
Well casing diameter change depth (m)	1781
Average well casing outer diameter d_B (m)	0.21
Depth of the 1st packer (m)	1000
Depth of the 2nd packer (m)	2763

Ammonia was selected as the working fluid, as the density of the steam phase is low enough that it can reach the surface without substantial pressure losses. In the analysed

case, where the temperature of the saturated steam in the heat exchange zone is 50 °C and neglecting any local losses due to pipe roughness, the pressure drops by about 1.9 bar and the temperature by about 3.5 °C, while the fluid flows to the surface. The vapourisation temperature changes depending on the depth, as the hydrostatic pressure rises along the depth of the well. For the temperatures and pressures of the analysed case, the vapourisation temperature increases from 50 to 55.26 °C from the top to the bottom of the borehole. The thermophysical properties of ammonia were gathered from the REFPROP database [26]. Because the model did not include fluid behaviour inside the well, the ammonia properties were used only for determining the increase in the vapourisation temperature and the decrease in temperature from the heat exchange zone to the turbine at the surface.

The calculation parameters used in the model are presented in Table 3 and Figure 2. The numerical model was implemented using Python 3.8. Figure 2 shows the modelled area with exaggerated borehole dimensions.

Table 3. Mathematical model parameters used in the calculations. The vapourisation temperature was calculated, while other parameters were determined empirically or are related to the dimensions of the analysed borehole.

Parameter	Value
Vapourisation temperature (°C)	50–55.26
Time horizon (a)	10
Time steps Δt (s)	1, 2, 3, 3.5 × 10^3
Time step change parameter	At every 100 time steps, extend the next time step. Last time step until the end.
Depth step Δz (m)	1
Radial distance step Δr (m)	0.105
Modelled area, depth (m)	2263
Modelled area, width	300

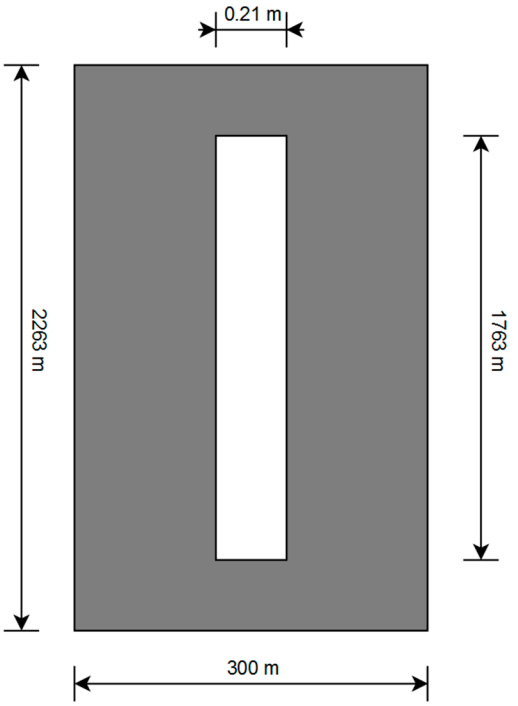

Figure 2. Modelled area with exact measurements of the borehole and its surroundings. The distances in the picture are exaggerated for clarity.

Ten years were chosen for the time horizon. The radial and depth distance steps were dependent on the borehole dimensions, where Δr should be, at most, half the diameter of the borehole so as to represent the volumes of the heat sinks inside the borehole and heat sources right outside the borehole casing's outside diameter accurately. Δz was chosen to be 1 m for the results to have a reasonable resolution. The greater the chosen distance steps, the faster the calculation will finish and the more stable it will be.

The analysed area was chosen based on the distant field radius described previously and the length of the previously described heat exchange area of the borehole.

3. Results and Discussion

The results of the model are presented and discussed in this section. Figure 3a,b present the undisturbed temperatures and the resulting temperatures in the surrounding formation after 10 years of operation at the maximum possible heat flow to the working fluid, respectively. The readily visible influence extends to about 50 m, with almost no change to the temperature at distances greater than 100 m. The analysed area has a super expressed depth dimension, making the plot of the whole area distorted. Figure 4 shows a closeup of the top (a) and the bottom (b) sections of the heat transfer area inside the borehole. The effect on the temperatures of the surroundings is uniform and symmetrical around the r axis, while the depth-dependent effect is not. This is a result of a positive heat flow possible from two extra adjacent temperature points at the top and bottom of the borehole, while, in the radial direction, the adjacent temperatures are appreciably higher only in the outward direction.

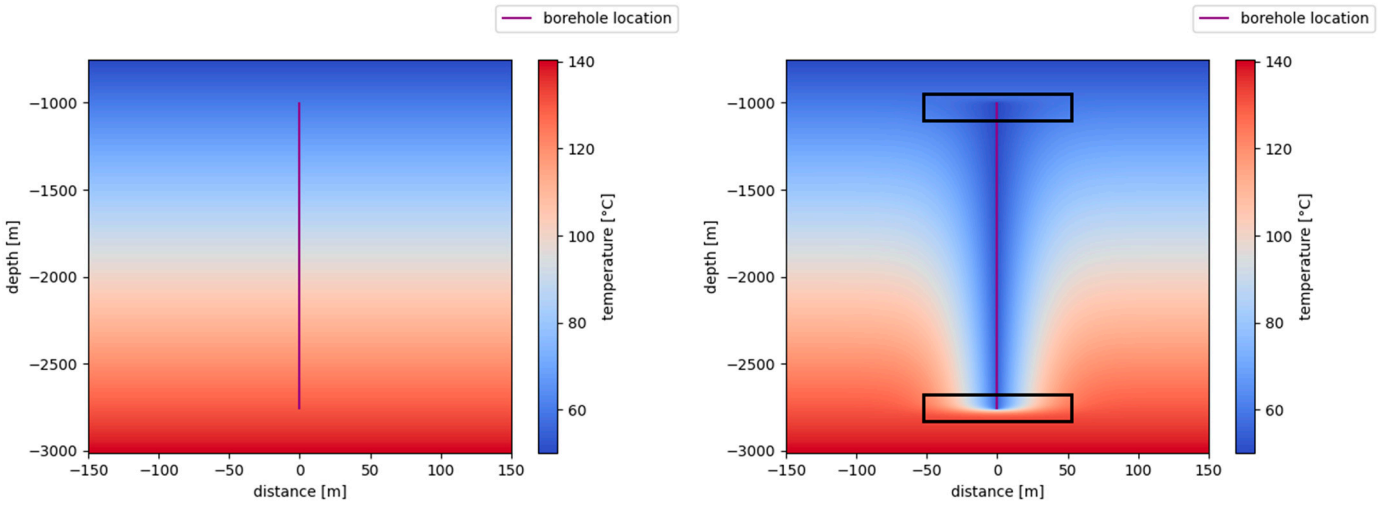

(**a**) (**b**)

Figure 3. Temperatures in the borehole surroundings: (**a**) undisturbed and (**b**) after 10 years of operation at maximum heat flow. The purple line represents the borehole, while the black squares in (**b**) show the closeup locations in Figure 4a,b.

It is expected that, because of the higher temperature gradient at the bottom of the heat exchange area, a greater amount of heat is going to be extracted from the surrounding rock formation than at the top. Consequently, the temperature difference should be greater at the bottom than at the top, with the same temperature drop occurring closer to the borehole than at the top.

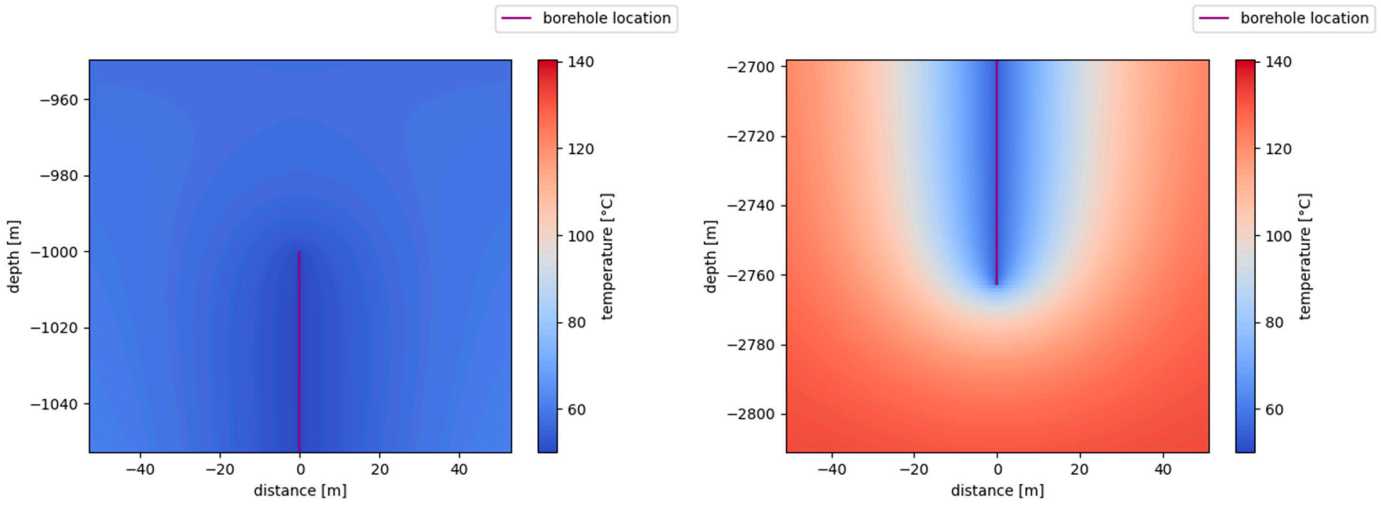

Figure 4. Temperatures in the borehole surroundings after 10 years of operation at maximum heat flow: (**a**) closeup of the bottom end of the heat exchange area and (**b**) closeup of the top end of the heat exchange area. The purple line shows the borehole location.

The effect is seen more prominently in Figure 5, where the temperature differences over the operating time are displayed instead of absolute values. The colour change corresponds to an order of magnitude change instead of a linear change. The formation temperature at a radial distance of 100 m or more changed by less than 0.1 °C over the operating time. The temperature change of the same magnitude extended farther with increasing the depth. There is a greater temperature difference in the radial direction than in the vertical direction, with the temperature change in the same order of magnitude occurring at about half the distance from the heat transfer area inside the borehole.

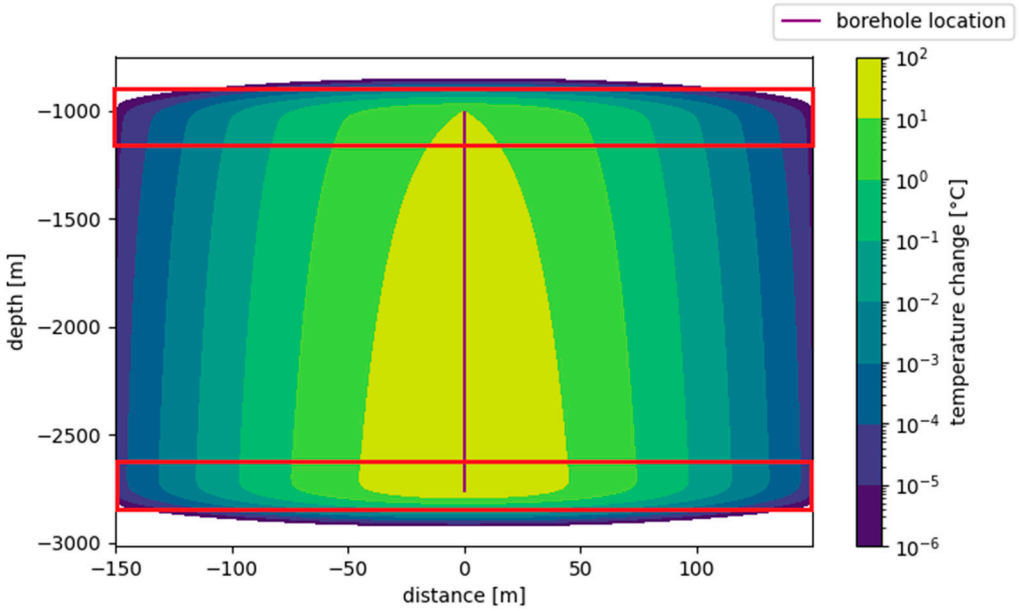

Figure 5. Relative temperature change in the surrounding formation after 10 years of operating at maximum heat flow. The red squares at the top and bottom of this figure show the closeup locations in Figure 6a,b.

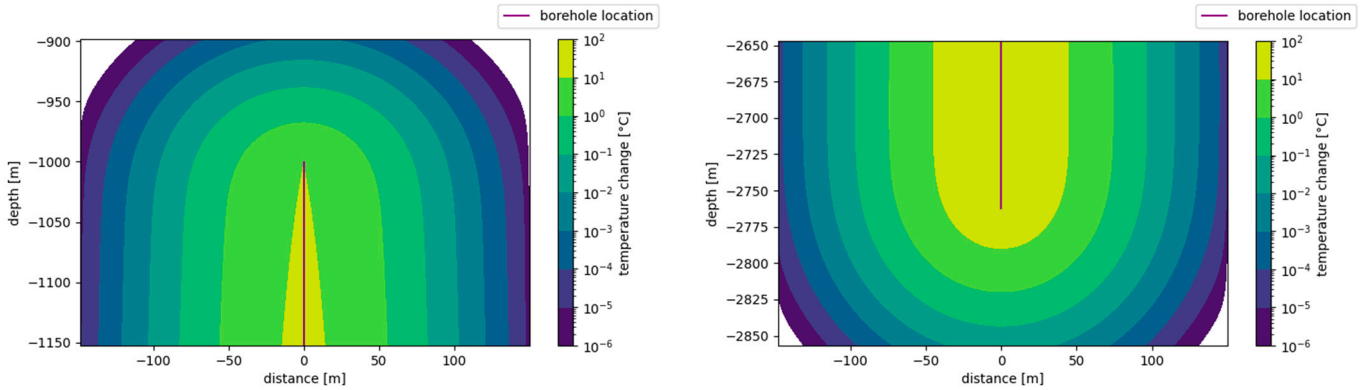

Figure 6. Relative temperature change in the surrounding formation after 10 years of operating at maximum heat flow: (**a**) closeup of the bottom end of the heat exchange area; (**b**) closeup of the top end of the heat exchange area.

This is more apparent in Figure 6, which displays a closeup of the top (a) and bottom (b) part of the heat exchange area. The top of the borehole had an initial temperature difference of 10 °C, which was reduced more rapidly than the higher temperature gradient at the bottom of the analysed area. The difference in radial heat flow and consequent temperature change between the top and the bottom of the borehole started to diminish farther from the borehole and became independent from the temperature of the working fluid.

Figure 7 displays the temperature profiles at three different depths of the analysed volume. The first graph presents the temperature profile at a depth of 1000 m or the exact top of the heat exchange area, the second graph is the temperature profile at a depth of 1881 m or the middle of the heat exchange area, and the last graph displays the temperature profile right after the heat exchange area or at 2763 m, respectively. The profile at 1881 m and 10 years hints at linearities in the temperature change, which is expected to develop at equilibrium conditions over a long enough period and within a limited volume. With the volume being unlimited, the profile will, after a long enough time, resemble a logarithmic curve with an asymptote at the initial conditions. After one month of operation, there was no change in temperature at a radial distance of 15 m at all of the depths shown, with a difference of 1 °C at 4 m, 4.5 m, and 5.985 m at the top, middle, and bottom temperature profiles, respectively. After one year, the radius of the affected temperature increased to 50 m for all depths, with the middle and bottom depths having the same radius of effect, while, at the top, the effect extended to 46.9 m.

A temperature difference of 1 °C occurred at almost the same distance of 21.6 m from the borehole for the bottom and middle profiles at 1 year of operation. The same difference at the top profile occurred 8.4 m closer to the well. The initial differences in depth-dependent surrounding and vapourisation temperatures equalised gradually through the vertical heat flow, while the majority of the heat still flowed towards the borehole in the horizontal direction. At 10 years of operation, the unaffected horizon moved to 150 m, with the top profile being only 3.15 m closer to the borehole. The 1 °C temperature change horizon was the same for the middle and bottom profiles at 68.1 m and the top profile at 43 m from the borehole. These trends suggest that the affected volume around the heat exchange area will, after an appreciable time, be symmetrical around the horizontal axis as well as the vertical one. The temperature gradient towards the borehole will differ depthwise, as the modelled surrounding formation has a directionless heat transfer coefficient. If there is a difference in the heat transfer coefficient in the z direction compared to the radial direction, for example, because of a vertical water flow, the thermal profile would be affected greatly [27].

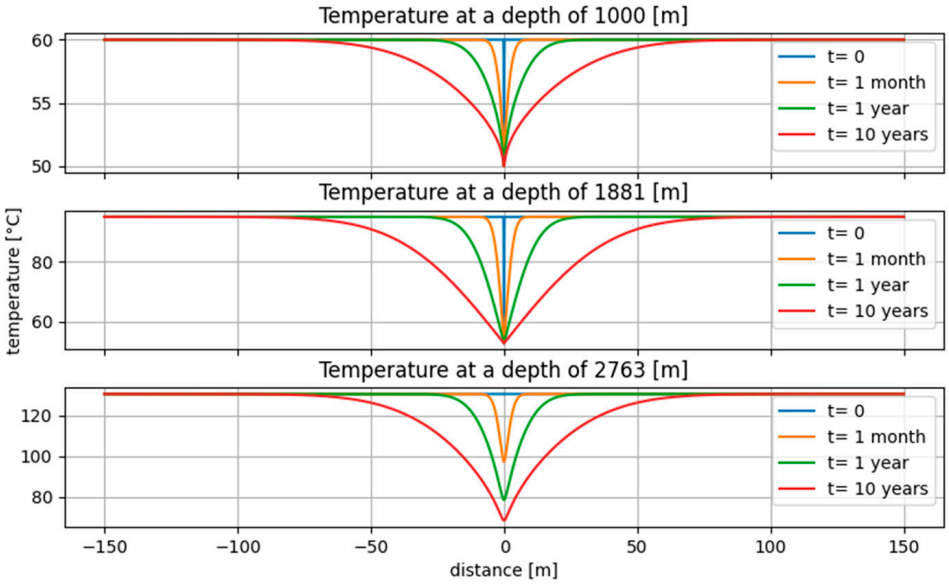

Figure 7. Temperature profiles at depths of 1000 m, 1881 m, and 2763 m before heat extraction and after 1 month, 1 year, and 10 years of maximum heat extraction. The temperature profile at 2763 m is just under the lowest point of the heat extracting chamber inside the borehole.

Figure 8 presents the maximum possible heat flow achievable with the analysed configuration for each time step. The heat flow was calculated for each point inside the borehole and then averaged over the entire volume of the heat exchange area. The maximum heat flow fell to 1/2 its starting value after 2.8 h and to 1/5 after a day of operation. The maximum heat flow trended towards 4 kW, with the last value equal to 4.01786 kW and only falling below 5 kW after 2337.2 days of operation, or 2.02×10^8 s. The sharp drop in the presented values is a consequence of the thermal conductivity of the surrounding formation. The slope of the curve would decrease slightly if the conductivity of the pipe inserted in the borehole was considered. The difference would be negligible and only visible at the start of operation, as the main resistance to heat flow originates from the bulk of the surrounding rock formation. The absolute heat flow values are directly proportional to the area over which the heat is conducted. The assumed asymptote and the starting value would increase but the shape of the curve would stay the same in the absence of any interactions between the areas of heat transfer.

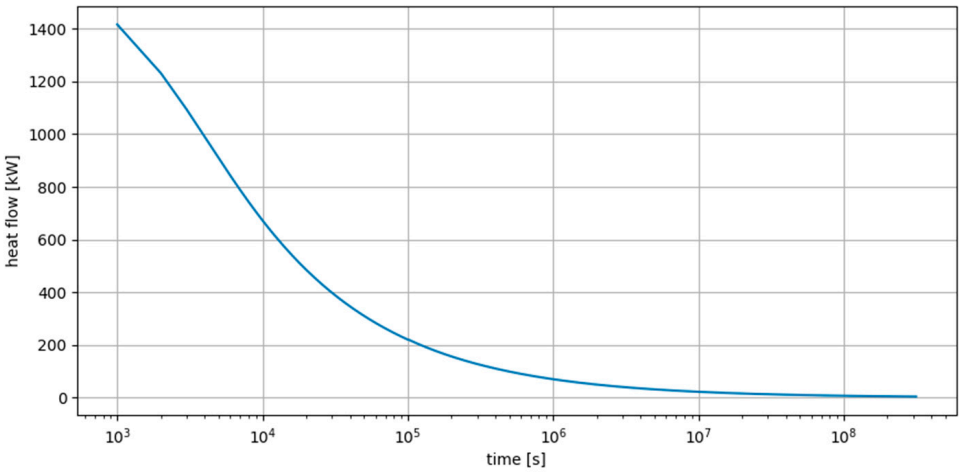

Figure 8. Change in maximum heat flow during 10 years of maximum heat extraction. The time axis is logarithmic to represent the nature of the heat flow decrease better during the operating timeline.

This type of heat extraction is inherently unsustainable. The heat flow decreases too rapidly to design an efficient system to transform or use the energy in the long term. With Carnot efficiencies at the temperatures used being around 10%, the energy generated would diminish quickly to unusable levels. The design of the system allows for operation at lower heat flows, as the vapourisation temperature is dependent only on the amount of the working fluid in the system, which would possibly extend the lifetime of stable continuous operation. A discontinuous type of operation could be employed, where the system could operate in 12 h cycles, to give the earth time to regenerate the spent heat. An asymmetrical cycle could be preferred, as only 86% of the temperature is regenerated after the same time period as the extraction time [28]. The heat available regenerates even slower, where 60% of the extracted heat is regenerated after an 8 times longer rest period than the extraction time [29].

4. Conclusions

This work describes a possible alternative use of abandoned oil and gas wells using a novel and patented heat exchanger, which can transport heat from deep underground to the surface without parasitic power consumption and at a constant temperature. A numerical model of the abandoned well surroundings is made using the equation for nonstationary heat flow in an infinite medium with negligible surface resistance. Point temperatures for the field and heat flow into the well were calculated and presented in graphical form. The results show that the rate of cooling in the surrounding formation is depth-dependent, while the radial extent of the effect on surrounding temperatures after the analysed time is not. The heat flow decreases rapidly to unusable levels if the extraction is conducted at maximum capacity and continuously. In future work, a sustainable heat flow could be calculated that can be extracted continuously over the operating time. If applicable, a discontinuous operation could be implemented, where the rated power will be higher than in sustainable continuous operation, while still keeping the extraction sustainable. If cost-effective installation, reliability, and longevity are realised in the development of this technology, the insights of this work could pave the way for future valourisation of abandoned wells.

Author Contributions: Conceptualisation, methodology, software, validation, formal analysis, investigation, resources, data curation, visualisation, project administration, writing—original draft preparation: U.G.; methodology, software, investigation, data curation: V.P.; writing—review and editing, supervision, funding acquisition: D.G. All authors have read and agreed to the published version of the manuscript.

Funding: This research was funded within the project "SI-Geo-Electricity—Pilot geothermal power plant on the existing gas well Pg-8, pilot project" no. C1541-22B710017. It is co-financed by Iceland, Liechtenstein, and Norway with the EGP Financial Mechanism resources in the amount of EUR 647,618.89 and the corresponding Slovenian participation in the amount of EUR 114,285.69. The purpose of the project is to increase renewable electricity by building the first pilot geothermal power plant in Slovenia.

Institutional Review Board Statement: Not applicable.

Informed Consent Statement: Not applicable.

Data Availability Statement: The data are contained within the article.

Acknowledgments: The authors of this paper thank Mojca Božič and Boštjan Gregorc (Dravske elektrarne Maribor d.o.o.) for providing the relevant well data, as well as Katarina Kores (University of Maribor) for guidance regarding the remote access of computing resources.

Conflicts of Interest: The funders had no role in the design of the study; in the collection, analyses, or interpretation of the data; in the writing of the manuscript; or in the decision to publish the results.

Abbreviations

GGHP	Geothermal Gravity Heat Pipe
LCOE	Levelised Cost of Electricity
NE	North-East
ORC	Organic Rankine Cycle
WBHX	Wellbore Heat Exchanger

References

1. Gupta, H.K.; Roy, S. *Geothermal Energy: An Alternative Resource for the 21st Century*; Elsevier: Amsterdam, The Netherlands, 2006; ISBN 978-0-08-046564-7.
2. Dye, S.T. Geoneutrinos and the Radioactive Power of the Earth. *Rev. Geophys.* **2012**, *50*, 1–19. [CrossRef]
3. Sharmin, T.; Khan, N.R.; Akram, M.S.; Ehsan, M.M. A State-of-the-Art Review on Geothermal Energy Extraction, Utilization, and Improvement Strategies: Conventional, Hybridized, and Enhanced Geothermal Systems. *Int. J. Thermofluids* **2023**, *18*, 100323. [CrossRef]
4. Davies, J.; Davies, D.R. Earth's Surface Heat Flux. *Solid Earth* **2010**, *1*, 5–24. [CrossRef]
5. Huttrer, G. *Geothermal Power Generation in the World 2015-2020 Update Report*; World Geothermal Congress: Reykjavik, Iceland, 2021.
6. Lund, J.W.; Toth, A.N. Direct Utilization of Geothermal Energy 2020 Worldwide Review. *Geothermics* **2021**, *90*, 101915. [CrossRef]
7. DiPippo, R. *Geothermal Power Plants: Principles, Applications, Case Studies and Environmental Impact*; Elsevier Science: Amsterdam, The Netherlands, 2015; ISBN 978-0-08-100282-7.
8. Soltani, M.; Moradi Kashkooli, F.; Souri, M.; Rafiei, B.; Jabarifar, M.; Gharali, K.; Nathwani, J.S. Environmental, Economic, and Social Impacts of Geothermal Energy Systems. *Renew. Sustain. Energy Rev.* **2021**, *140*, 110750. [CrossRef]
9. Bravi, M.; Basosi, R. Environmental Impact of Electricity from Selected Geothermal Power Plants in Italy. *J. Clean. Prod.* **2014**, *66*, 301–308. [CrossRef]
10. Templeton, J.D.; Ghoreishi-Madiseh, S.A.; Hassani, F.; Al-Khawaja, M.J. Abandoned Petroleum Wells as Sustainable Sources of Geothermal Energy. *Energy* **2014**, *70*, 366–373. [CrossRef]
11. Alimonti, C.; Soldo, E.; Bocchetti, D.; Berardi, D. The Wellbore Heat Exchangers: A Technical Review. *Renew. Energy* **2018**, *123*, 353–381. [CrossRef]
12. Le Lous, M.; Larroque, F.; Dupuy, A.; Moignard, A. Thermal Performance of a Deep Borehole Heat Exchanger: Insights from a Synthetic Coupled Heat and Flow Model. *Geothermics* **2015**, *57*, 157–172. [CrossRef]
13. Sohani, A.; Mohammadian, A.; Asgari, N.; Samiezadeh, S.; Doranehgard, M.H.; Goodarzi, E.; Nastasi, B.; Garcia, D.A. 8—Simulation and Thermodynamic Modeling of Heat Extraction from Abandoned Wells. In *Utilization of Thermal Potential of Abandoned Wells*; Noorollahi, Y., Naseer, M.N., Siddiqi, M.M., Eds.; Academic Press: Cambridge, MA, USA, 2022; pp. 135–155. ISBN 978-0-323-90616-6.
14. Harris, B.E.; Lightstone, M.F.; Reitsma, S. A Numerical Investigation into the Use of Directionally Drilled Wells for the Extraction of Geothermal Energy from Abandoned Oil and Gas Wells. *Geothermics* **2021**, *90*, 101994. [CrossRef]
15. Liu, Z.; Yang, W.; Xu, K.; Zhang, Q.; Yan, L.; Li, B.; Cai, X.; Yang, M. Research Progress of Technologies and Numerical Simulations in Exploiting Geothermal Energy from Abandoned Wells: A Review. *Geoenergy Sci. Eng.* **2023**, *224*, 211624. [CrossRef]
16. Cheng, W.-L.; Li, T.-T.; Nian, Y.-L.; Xie, K. Evaluation of Working Fluids for Geothermal Power Generation from Abandoned Oil Wells. *Appl. Energy* **2014**, *118*, 238–245. [CrossRef]
17. Falcone, G.; Liu, X.; Okech, R.R.; Seyidov, F.; Teodoriu, C. Assessment of Deep Geothermal Energy Exploitation Methods: The Need for Novel Single-Well Solutions. *Energy* **2018**, *160*, 54–63. [CrossRef]
18. Goričanec, D.; Krope, J.; Tomšič, L. Gravitational Heat Pipe for the Production of Geothermal Heat 2012. Available online: https://patents.google.com/patent/SI23618A/en (accessed on 27 May 2024).
19. Pilot Geothermal Power Plant on the Existing Pg-8 Gas Well. Available online: https://si-geo-electricity.si/en/home-english/ (accessed on 13 July 2023).
20. Levenspiel, O. *Engineering Flow and Heat Exchange*; Springer: Boston, MA, USA, 2014; ISBN 978-1-4899-7453-2.
21. Eberly, D. Stability Analysis for Systems of Differential Equations. 2008. Available online: https://www.geometrictools.com/Documentation/StabilityAnalysis.pdf (accessed on 27 May 2024).
22. Hart, D.P.; Couvillion, R. *Earth-Coupled Heat Transfer: Offers Engineers and Other Practitioners of Applied Physics the Information to Solve Heat Transfer Problems as They Apply to Earth-Coupling*; National Water Well Association: Dublin, OH, USA, 1986.
23. eGeologija—Geološki Zavod Slovenije. Available online: https://egeologija.si/geonetwork/srv/eng/catalog.search#/home (accessed on 14 March 2024).
24. Šram, D.; Rman, N.; Rižnar, I.; Lapanje, A. The Three-Dimensional Regional Geological Model of the Mura-Zala Basin, Northeastern Slovenia. *Geologija* **2015**, *58*, 139–154. [CrossRef]
25. Rajver, D.; Adrinek, S. Overview of the Thermal Properties of Rocks and Sediments in Slovenia. *Geologija* **2023**, *66*, 125–150. [CrossRef]
26. Reference Fluid Thermodynamic and Transport Properties Database (REFPROP). Available online: https://www.nist.gov/programs-projects/reference-fluid-thermodynamic-and-transport-properties-database-refprop (accessed on 27 May 2024).

27. Saeid, S.; Al-Khoury, R.; Barends, F. An Efficient Computational Model for Deep Low-Enthalpy Geothermal Systems. *Comput. Geosci.* **2013**, *51*, 400–409. [CrossRef]
28. Pokhrel, S.; Sasmito, A.P.; Sainoki, A.; Tosha, T.; Tanaka, T.; Nagai, C.; Ghoreishi-Madiseh, S.A. Field-Scale Experimental and Numerical Analysis of a Downhole Coaxial Heat Exchanger for Geothermal Energy Production. *Renew. Energy* **2022**, *182*, 521–535. [CrossRef]
29. Hage Meany, B. Modelling and Simulation for Optimizing Adeep, Closed-Loop Geothermal Heat Exchangesystem. 2018. Available online: https://www.semanticscholar.org/paper/Modelling-and-simulation-for-optimizing-adeep,-heat-Meany/6258d75d21e10727e6c2b46a7881c41cb1194a5b (accessed on 27 May 2024).